Enhanced blue emission from Tm-doped $Al_xGa_{1-x}N$ electroluminescent thin films

D. S. Lee and A. J. Steckl[a)]
Nanoelectronics Laboratory, University of Cincinnati, Cincinnati, Ohio 45221-0030

(Received 4 April 2003; accepted 30 July 2003)

Electroluminescent (EL) emission from Tm-doped $Al_xGa_{1-x}N$ ($Al_xGa_{1-x}N$:Tm) has been observed with various Al compositions ($0 \leqslant x \leqslant 1$). $Al_xGa_{1-x}N$:Tm thin films were grown by molecular beam epitaxy with *in situ* doping of Tm. At lower Al composition ($x < 0.15$), blue emission at 478 nm dominates, corresponding to the Tm $^1G_4 \rightarrow {}^3H_6$ transition. For $x > 0.15$, however, a second blue emission peak was observed at 465 nm, becoming dominant with increasing Al composition. The 465 nm emission is attributed to the higher level Tm transition $^1D_2 \rightarrow {}^3F_4$, which was not observed in GaN:Tm. Blue EL emission from Tm was enhanced with Al content in the films. The ratio of EL intensity at blue (465 nm plus 478 nm) to infrared (801 nm) wavelengths increased monotonically with Al composition, from ~2 for GaN:Tm to ~30 for AlN:Tm. © *2003 American Institute of Physics.* [DOI: 10.1063/1.1611275]

A major challenge[1,2] of electroluminescent devices (ELDs) has been to obtain bright blue emission, which carries the highest energy per photon (2.6–2.7 eV) of the three primary colors. Tm-doped II–VI materials, including ZnS, have been widely studied[3–5] for blue emission but have yielded relatively weak blue EL emission at ~480 nm and strong IR emission at ~800 nm. We have investigated[6] the wide band gap III–V semiconductor GaN as a host for thin film electroluminescent (TFEL) devices, previously reporting[7] dominant blue EL emission from GaN:Tm. Moreover, we have investigated several methods for enhancement of blue emission from GaN:Tm ELDs in both brightness and efficiency, including the ''photopumping'' method[8] and control[9] of the growth temperature. The mixed III–V alloys of GaN–AlN span a large band gap energy range from 3.4 to 6.2 eV. Introducing AlN in GaN films doped with Er has been shown[10] to improve TFEL device performance. Furthermore, AlN doped with Er, Eu, and Tb has resulted in photoluminescence[11] and cathodoluminescence,[12,13] and EL has been reported for AlN:Er.[14] In this letter we report on the growth of *in situ* Tm-doped $Al_xGa_{1-x}N$ films and the corresponding effect of Al composition on the EL emission.

$Al_xGa_{1-x}N$:Tm films were grown on *p*-type (111) Si substrates by molecular beam epitaxy with a Ga elemental source and a nitrogen plasma source. Doping was performed *in situ* during growth from a solid Tm source. The Tm cell temperature was fixed at 600 °C resulting in a concentration between ~0.2 and ~0.5 at. %. $Al_xGa_{1-x}N$:Tm layers were typically grown for 1 h at 550 °C with a growth rate of 0.5–0.6 μm/h. Films were grown with various Al compositions ($0 \leqslant x \leqslant 1$). The growth was performed under slightly N-rich growth conditions: 1.5 sccm for nitrogen flow rate and 400 W for plasma power. Al composition was controlled by varying the Al cell temperature during growth. The total flux of group III species (Ga and Al) was kept constant (by adjusting both Ga and Al cell temperatures) since EL properties are reported[15] to be a strong function of V/III ratio during growth. Al composition was determined by the x-ray diffraction method. According to Vegard's law,[16,17] the (0002) peak of $Al_xGa_{1-x}N$ is a linear function of Al composition between GaN and AlN. We grew films with various Al compositions including $x = 0$ (GaN), 0.16, 0.21, 0.39, 0.62, 0.81, and 1 (AlN). Ring-shaped Schottky diodes were fabricated for EL measurements using indium tin oxide sputtering and a lift-off process. The fabrication and operation of EL devices have been previously reported.[18]

Figure 1 shows the EL emission spectrum from an AlN:Tm ELD. Negative 120 V dc bias was applied and current flow was ~68 μA, which is about two orders of magnitude more resistive than GaN:Tm films under a similar bias condition. Major EL emission peaks were observed in the UV region (371 nm), the blue region (465 and 478 nm), and the IR (802 nm). The 478 and 802 nm emissions are well-

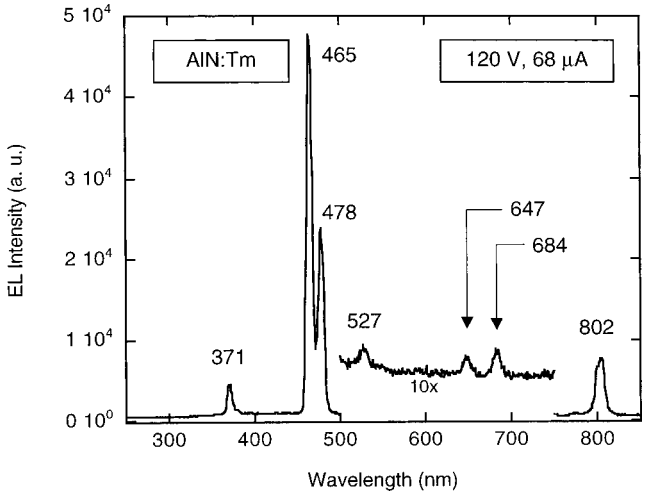

FIG. 1. EL emission spectrum from an ELD on AlN:Tm film under a negative bias 120 V, ~68 μA. Strong EL emissions are observed at 371, 465, 478, and 802 nm. Weak emissions are also detected at 527, 647, and 682 nm. The 371 and 465 nm emission lines have not been previously observed in GaN:Tm.

a)Electronic mail: a.steckl@uc.edu

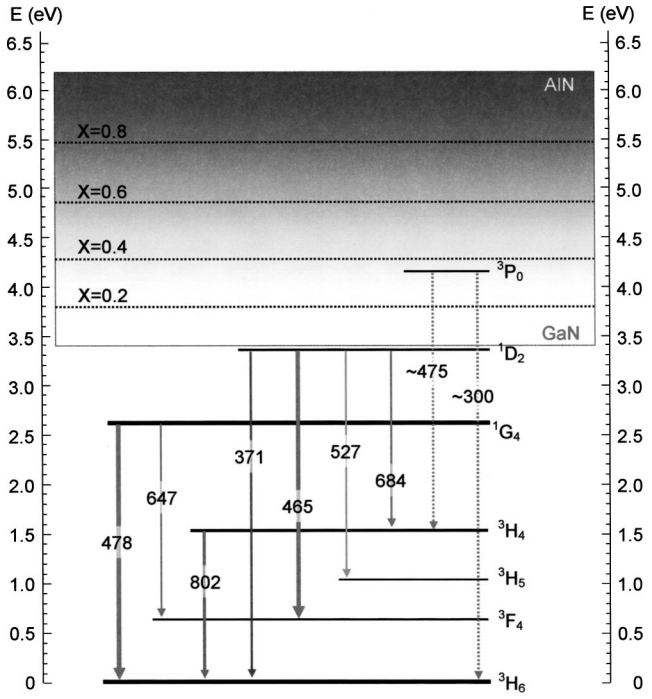

FIG. 2. Diagram of energy levels and $4f-4f$ inner shell transitions of Tm^{3+} in $Al_xGa_{1-x}N$:Tm. Note that the observed emission lines at 371, 465, 527, and 684 nm were attributed to the transitions $^1D_2 \rightarrow {}^3H_6$, $^1D_2 \rightarrow {}^3F_4$, $^1D_2 \rightarrow {}^3H_5$, and $^1D_2 \rightarrow {}^3H_4$, respectively.

known and attributed to $^1G_4 \rightarrow {}^3H_6$ and $^3H_4 \rightarrow {}^3H_6$ transitions, respectively. The 371 and 465 nm peaks are not present in GaN:Tm ELDs. Minor peaks were also detected at 527, 647, and 682 nm. We have reported[9] that the 647 nm emission observed in GaN:Tm is due to the $^1G_4 \rightarrow {}^3F_4$ transition. The 527 and 684 nm peaks were not seen in GaN:Tm ELDs. Note that $^3F_4$ and $^3H_4$ are frequently reversed in the literatures. The 465 nm emission is the focus of this work, since it leads to the emission enhancement of blue in $Al_xGa_{1-x}N$:Tm ELDs.

The energy levels of $4f-4f$ inner shell transitions of Tm^{3+} in $Al_xGa_{1-x}N$:Tm are shown in Fig. 2. The band gap energy in various $Al_xGa_{1-x}N$ alloy compositions from 0.2 to 0.8 is shown according to Vegard's law taking a bowing parameter into account. Many different groups reported[16,17,19,20] as many different values for the bowing parameter, from $b=0.25$ to 2.1. Here we use $b=1$, which is close to the average of those values. We have attempted an attribution of the transitions for the emissions at 371, 465, 527, and 684 nm. We believe that they are due to $^1D_2 \rightarrow {}^3H_6$, $^1D_2 \rightarrow {}^3F_4$, $^1D_2 \rightarrow {}^3H_5$, and $^1D_2 \rightarrow {}^3H_4$, respectively. The $^3P_0 \rightarrow {}^3H_4$ transition was ruled out as the source of the 465 nm emission for several reasons. (1) Even though the $^3P_0$ level lies at ~4.16 eV (equivalent to the band gap of $Al_{0.35}Ga_{0.65}N$), 465 nm emission can be observed at $x<0.2$. A very small 465 nm peak is present at $x=0.16$ (see Fig. 3) and the peak becomes very clear at $x=0.21$ (not shown here). (2) Other groups reported similar blue emissions from various oxides[21–23] through upconversion, which were observed at shorter wavelength than that of $^1G_4 \rightarrow {}^3H_6$ transition and were attributed to the $^1D_2 \rightarrow {}^3F_4$ transition.

The $Al_xGa_{1-x}N$:Tm EL spectra were found to change significantly with Al composition. Figure 3 shows a series of

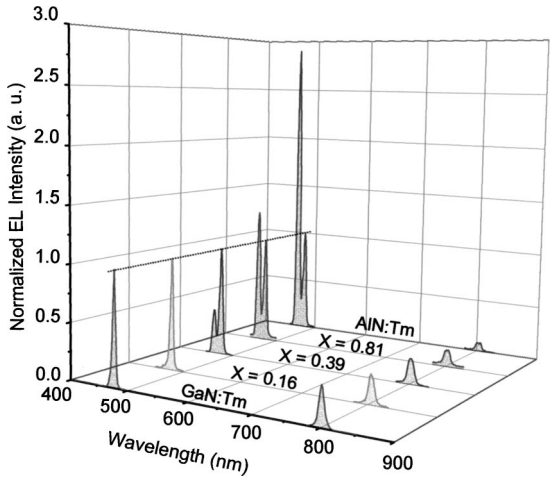

FIG. 3. EL spectra of $Al_xGa_{1-x}N$:Tm films with various Al compositions. Each EL spectrum was normalized by its current flow and then normalized once again by its intensity at 478 nm. A dotted line along 478 nm peaks is shown for guidance. The 465 nm emission becomes stronger with increasing Al composition while the 802 nm emission decreases.

EL spectra for various Al compositions. Each EL spectrum was first normalized by the ELD current flow to provide a meaningful basis for comparison. Then each spectrum was normalized by its intensity at 478 nm in order to highlight the comparison between 465 and 478 nm emissions as a function of Al composition. A dotted line is drawn along the 478 nm peaks as guidance. The 465 nm emission is barely present at $x=0.16$, it becomes very clear for $x \geqslant 0.39$, and it dominates for $x \geqslant 0.81$. The EL emission at 802 nm experienced the opposite trend, decreasing with Al composition. This pattern indicates that increasing the Al composition results in increasing efficiency for higher-level blue emission (465 nm) at the expense of the lower energy IR emission. This is reasonable, since the wider band gap can accommodate higher energy levels of Tm ions and provides a larger energy difference between hot electrons in the conduction band and the Tm excited states.

The integrated EL intensity of blue (both 465 and 478

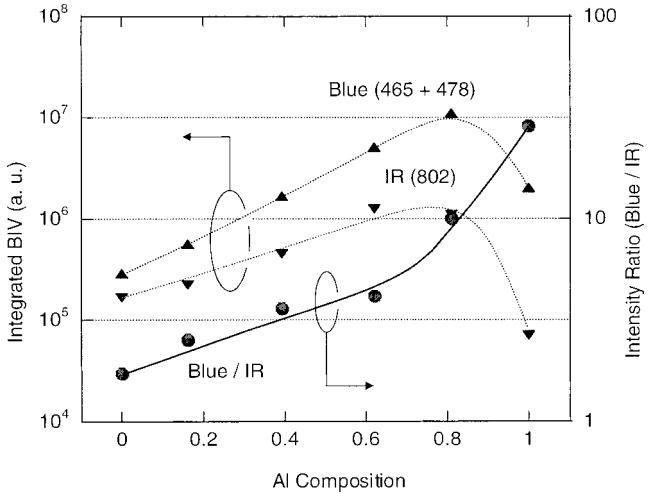

FIG. 4. Plot of integrated EL intensity (BIV) of combined blue (@465 nm+@478 nm) and IR (@ 802 nm) vs Al composition. Both blue and IR EL intensity increase with Al composition, except for the case of AlN:Tm. Intensity ratio (blue/IR) monotonically increases, from ~2 for GaN:Tm to ~30 for AlN:Tm.

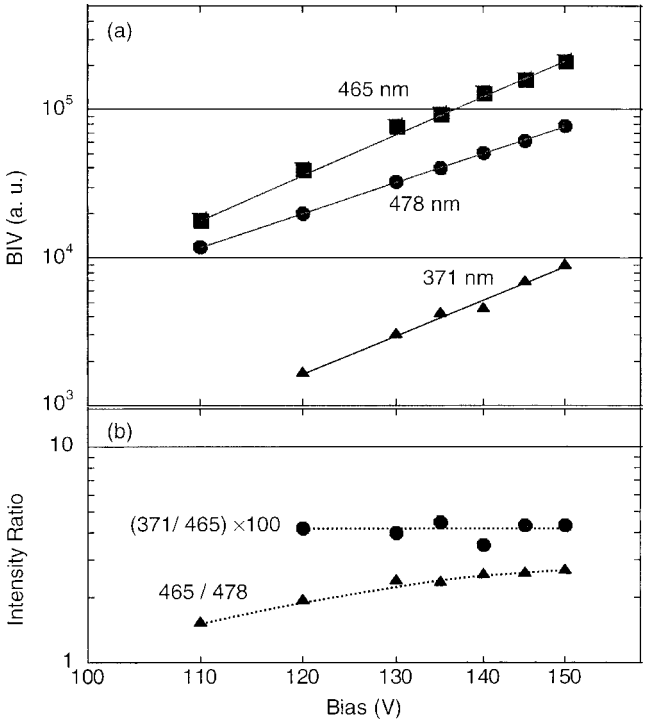

FIG. 5. (a) Plot of EL emission intensity (BIV) vs applied bias. EL intensities have power dependence with bias ($\propto V^n$). (b) Plot of intensity ratios vs applied bias. Note that the constant behavior of the 371/465 ratio indicates that both 371 and 465 nm emission lines originate from the same energy level, namely $^1D_2$.

nm) and IR (802 nm) are plotted versus Al composition in Fig. 4. We used current-normalized EL intensity[24] (BIV) instead of raw intensity in order to minimize the influence from many factors including those associated with EL device fabrication. Both blue and IR EL intensity increase with Al composition up to $x=0.8$, but decrease for AlN:Tm. The intensity ratio (blue/IR) monotonically increases, from ~ 2 for GaN:Tm to ~ 30 for AlN:Tm. Reduced intensity from AlN:Tm could be due to the extremely resistive nature of AlN:Tm.

The effect of applied voltage on the EL emission intensity at several emission wavelengths (371, 465, and 478 nm) is shown in Fig. 5. All emission peaks show the same trend, increasing monotonically with bias in Fig. 5(a). The EL intensities exhibit a power dependence with bias ($\propto V^n$), and $n=7.5$, 7.8, and 6.0, at the three wavelengths. As previously reported,[3,9] this indicates that the major emission mechanism is direct impact excitation of Tm^{3+} by hot electrons. The emission intensity ratios show two very interesting trend with bias: the 371/465 ratio is constant, while the 465/478 ratio monotonically increases. The constant behavior of the 371/465 ratio strongly indicates that both 371 and 465 nm emission lines originate from the same energy level, namely $^1D_2$.

In summary, we have obtained enhanced blue EL emission from $Al_xGa_{1-x}N$:Tm, especially, AlN:Tm. Increasing the band gap enabled the excitation of a second blue line attributed to the $^1D_2 \rightarrow {}^3H_6$ transition. The 465 nm emission, which was not observed in GaN:Tm, starts to appear $x > 0.15$ and becomes dominant with increasing Al composition. Both EL intensity (combined blue and IR) and its ratio (combined blue/IR) monotonically increase with Al composition, with the intensity ratio reaching ~ 30 for AlN:Tm. We have confirmed that blue EL emission becomes dominant over IR emission with increasing Al composition in the $Al_xGa_{1-x}N$ host.

This work was supported by ARO and ARL grants. The authors are pleased to acknowledge the support of E. Forsythe, D. Morton, and J. Zavada.

[1] C. N. King, J. Vac. Sci. Technol. A **14**, 1729 (1996).
[2] R. H. Mauch, Appl. Surf. Sci. **92**, 589 (1996).
[3] J. M. Sun, G. Z. Zhong, X. W. Fan, C. W. Zheng, G. O. Mueller, and R. Mueller-Mach, J. Appl. Phys. **83**, 3374 (1998).
[4] S. H. Sohn and Y. Hamakawa, Appl. Phys. Lett. **62**, 2242 (1993).
[5] P. D. Keir, C. Maddix, B. A. Baukol, J. F. Wager, B. L. Clark, and D. A. Keszler, J. Appl. Phys. **86**, 6810 (1999).
[6] A. J. Steckl, J. C. Heikenfeld, D. S. Lee, M. J. Garter, C. C. Baker, Y. Wang, and R. Jones, IEEE J. Sel. Top. Quantum Electron. **8**, 749 (2002).
[7] A. J. Steckl, M. Garter, D. S. Lee, J. Heikenfeld, and R. Birkhahn, Appl. Phys. Lett. **75**, 2184 (1999).
[8] D. S. Lee and A. J. Steckl, Appl. Phys. Lett. **81**, 2331 (2002).
[9] D. S. Lee and A. J. Steckl, Appl. Phys. Lett. **82**, 55 (2003).
[10] J. Heikenfeld and A. J. Steckl, Mater. Res. Soc. Symp. Proc. **639**, G10.4.1 (2001).
[11] X. Wu, U. Hömmerich, J. D. Mackenzie, C. R. Abernathy, S. J. Pearton, R. N. Schwartz, R. G. Wilson, and J. M. Zavada, Appl. Phys. Lett. **70**, 2126 (1997).
[12] W. M. Jadwisienczak, H. J. Lozykowski, I. Berishev, A. Bensaoula, and I. G. Brown, J. Appl. Phys. **89**, 4384 (2001).
[13] K. Gurumurugan, H. Chen, G. R. Harp, W. M. Jadwisienczak, and H. J. Lozykowski, Appl. Phys. Lett. **74**, 3008 (1999).
[14] V. I. Dimitrova, P. G. Van Patten, H. H. Richardson, and M. E. Kordesh, Appl. Phys. Lett. **77**, 478 (2000).
[15] D. S. Lee and A. J. Steckl, Appl. Phys. Lett. **80**, 728 (2002).
[16] M. Stutzmann, O. Ambacher, A. Cros, M. S. Brandt, H. Angerer, R. Dimitrov, N. Reinacher, T. Metzger, R. Höpler, D. Brunner, F. Freudenberg, and R. Handschuh, Mater. Sci. Eng., B **50**, 212 (1997).
[17] N. Teofilov, K. Thonke, R. Sauer, L. Kirste, D. G. Ebling, and K. W. Benz, Diamond Relat. Mater. **11**, 892 (2002).
[18] M. J. Garter and A. J. Steckl, IEEE Trans. Electron Devices **49**, 48 (2002).
[19] I.-H. Lee and Y. Park, Phys. Status Solidi A **192**, 67 (2002).
[20] D. G. Ebling, L. Kirste, K. W. Benz, N. Teofilov, K. Thonke, and R. Sauer, J. Cryst. Growth **227–228**, 453 (2001).
[21] J. B. Gruber, A. O. Wright, M. D. Seltzer, B. Zandi, L. D. Merkle, J. A. Hutchinson, C. A. Morrison, T. H. Allik, and B. H. T. Chai, J. Appl. Phys. **81**, 6585 (1997).
[22] J. R. Bonar, M. V. D. Vermelho, A. J. McLaughlin, P. V. S. Marques, J. S. Aitchison, J. F. Martins-Filho, A. G. Bezerra-Jr., A. S. L. Gomes, and C. B. de Araujo, Opt. Commun. **141**, 137 (1997).
[23] S. Kishimoto and K. Hirao, J. Non-Cryst. Solids **213&214**, 393 (1997).
[24] D. S. Lee, J. Heikenfeld, A. J. Steckl, U. Hommerich, J. T. Seo, A. Braud, and J. Zavada, Appl. Phys. Lett. **79**, 719 (2001).